TMLAI TRANSACTIONS ON MACHINE LEARNING AND ARTIFICIAL INTELLIGENCE
SOCIETY FOR SCIENCE AND EDUCATION UNITED KINGDOM
Volume 8 No 4
ISSN 2054-7390

A Block Diagram of Electromagnetoelastic Actuator for Control Systems in Nanoscience and Nanotechnology

Sergey Mikhailovich Afonin
National Research University of Electronic Technology (MIET), Moscow, Russia;
eduems@mail.ru

ABSTRACT

The block diagram and the transfer functions of the electromagnetoelastic actuator are received for control systems in nanoscience and nanotechnology. The block diagram of the electromagnetoelastic actuator is reflected the transformation of electrical energy into mechanical energy, in contrast to Cady's and Mason's electrical equivalent circuits of piezotransducer. The electromagnetoelasticity equation and the second order linear ordinary differential equation with boundary conditions are solved for calculations the block diagram of the electromagnetoelastic actuator. The block diagram of the piezoactuator is obtained with using the reverse and direct piezoelectric effects. The back electromotive force is determined from the direct piezoelectric effect equation. The transfer functions of the piezoactuators are obtained for control systems in nanoscience and nanotechnology.

Keywords: Block diagram; Electromagnetoelastic actuator; Piezoactuator; Nanoscience; Nanotechnology; Transfer function.

1 Introduction

The block diagram of the electromagnetoelastic actuator is reflected the transformation of the electrical energy into the mechanical energy, in contrast to Cady's and Mason's electrical equivalent circuits of the piezotransducer, the vibration piezomotor [1 – 14]. The block diagram of electromagnetoelastic actuator for control systems in nanoscience and nanotechnology is obtained with the mechanical parameters the displacement and the force [7 – 9, 13, 14]. The electromagnetoelastic actuator with the piezoelectric or magnetostriction effect is used for precise alignment in nanoscience and nanotechnology, the adaptive optics, the laser systems, the communications systems, the nanobiomedical research.

The block diagram of the electromagnetoelastic actuator is obtained by solved the electromagnetoelasticity equation and the second order linear ordinary differential equation with boundary conditions. The block diagram of the piezoactuator is received with considering the reverse and direct piezoelectric effects. The back electromotive force is obtained from the direct piezoelectric effect equation. For calculate control systems with electromagnetoelastic actuator in nanoscience and nanotechnology the block diagram and diagram and transfer functions of the electromagnetoelastic actuator are received.

The piezoactuator for the nanodisplacement based on the inverse piezoeffect. The piezoactuator is used in the nanomanipulator for scanning microscopy . The nanomanipulator with the piezoactuator is key

DOI: 10.14738/tmlai.84.8476
Publication Date: 26th June, 2020
URL: http://dx.doi.org/10.14738/tmlai.84.8476

component in the nanomechatronics systems for nanoscience, nanotechnology and nanobiomedical research [15 − 30].

The electromagnetoelastic actuator is the electromechanical device intended for actuation of mechanisms, systems or management based on the electromagnetoelasticity effect, converts the electrical signals into the mechanical movement or the force [13 − 18].

The electromagnetoelastic actuator is provided displacement 1 nm - 10 μm, force 1000 N, response 1-10 ms. The transfer functions of the electromagnetoelastic actuators are obtained from its block diagram for nanoscience and nanotechnology. The characteristics of the electromagnetoelastic actuator are received for the calculation the nanomechatronics systems in nanoscience and nanotechnology.

2 Block diagram and transfer functions of actuator

The block diagram and the matrix transfer functions of the electromagnetoelastic actuator for control systems in nanoscience and nanotechnology are obtained from the structural-parametric model of the electromagnetoelastic actuator with the mechanical parameters the displacement and the force. The block diagrams of the piezoactuator are determined from the structural model of the electromagnetoelastic actuator [7 – 9, 13, 14].

The equation of electromagnetoelasticity [7 – 9, 11, 13, 14, 23, 24] for separately effect the electric field strength and the magnetic field strength is obtained in the form of the reverse effect for the actuator

$$S_i = d_{mi}\Psi_m + s_{ij}^{\Psi}T_j\,, \tag{1}$$

where S_i is the relative displacement of the electromagnetoelastic actuator; d_{mi} is the coefficient of the electromagnetoelasticity in the form piezomodule or the coefficient of magnetostriction; Ψ_m is the control parameter in the form electric E_m or magnetic H_m field strength; s_{ij}^{Ψ} is the elastic compliance at $\Psi = \text{const}$; T_j is the mechanical stress; $i, j = 1, 2, \ldots, 6$, $m = 1, 2, 3$ are the indexes.

The equation of the forces at the faces of the electromagnetoelastic actuator is received in the form

$$TS_0 = F + M\frac{d^2\xi(x,t)}{dt^2}\,, \tag{2}$$

where F, M are the force and the mass.

The second order linear ordinary differential equation for the electromagnetoelastic actuator is obtained by using the Laplace transform to the wave equation and setting the initial conditions to zero. The second order linear ordinary differential equation [8, 11, 13, 14, 23, 26, 28] has the following form

$$\frac{d^2\Xi(x,s)}{dx^2} - \gamma^2\Xi(x,s) = 0\,. \tag{3}$$

Therefore, solution (3) has the form

$$\Xi(x,s) = Ce^{-x\gamma} + Be^{x\gamma}\,, \tag{4}$$

$$\gamma = s/c^{\Psi} + \alpha\,, \tag{5}$$

where $\Xi(x,s)$, x, s are the Laplace transform for the displacement of the actuator, the coordinate, the Laplace operator; *C* and *B* are the coefficients; γ is the wave propagation coefficient; c^{Ψ} is the speed of sound in the actuator at $\Psi = \text{const}$; α is the attenuation coefficient.

The system of the equations is denoted for the faces of the actuator

$$\Xi(0,s) = \Xi_1(s) \quad \text{for} \quad x = 0; \tag{6}$$

$$\Xi(l,s) = \Xi_2(s) \quad \text{for} \quad x = l.$$

From (4), (6) the coefficients C and B have the form

$$C = \left(\Xi_1 e^{l\gamma} - \Xi_2\right) / \left[2\text{sh}(l\gamma)\right], \quad B = \left(\Xi_2 - \Xi_1 e^{-l\gamma}\right) / \left[2\text{sh}(l\gamma)\right]. \tag{7}$$

Therefore, the solution (3) has the form

$$\Xi(x,s) = \left\{\Xi_1(s)\text{sh}\left[(l-x)\gamma\right] + \Xi_2(s)\text{sh}(x\gamma)\right\} / \text{sh}(l\gamma). \tag{8}$$

The Laplace transform of the system of the equations for the forces acting on the faces the electromagnetoelastic actuator are received from (2) in the form

$$T_j(0,s)S_0 = F_1(s) + M_1 s^2 \Xi_1(s) \quad \text{for} \quad x = 0; \tag{9}$$

$$T_j(l,s)S_0 = -F_2(s) - M_2 s^2 \Xi_2(s) \quad \text{for} \quad x = l,$$

where S_0 is the area of the actuator.

The system of the equations for the Laplace transform of the mechanical stresses on the faces of the electromagnetoelastic actuator is obtained from (1) at $x = 0$ and $x = l$ in the form

$$T_j(0,s) = \frac{1}{s_{ij}^{\Psi}} \frac{d\Xi(x,s)}{dx}\bigg|_{x=0} - \frac{d_{mi}}{s_{ij}^{\Psi}} \Psi_m(s); \tag{10}$$

$$T_j(l,s) = \frac{1}{s_{ij}^{\Psi}} \frac{d\Xi(x,s)}{dx}\bigg|_{x=l} - \frac{d_{mi}}{s_{ij}^{\Psi}} \Psi_m(s).$$

The system of the equations for the structural model and the block diagram of the electromagnetoelastic actuator on Figure 1 are received from the equations (9), (10) in the form

$$\Xi_1(s) = \left[1/\left(M_1 s^2\right)\right]\left\{\begin{array}{l} -F_1(s) + \left(1/\chi_{ij}^{\Psi}\right) \\ \times \left[d_{mi}\Psi_m(s) - \left[\gamma/\text{sh}(l\gamma)\right]\left[\text{ch}(l\gamma)\Xi_1(s) - \Xi_2(s)\right]\right] \end{array}\right\}; \tag{11}$$

$$\Xi_2(s) = \left[1/\left(M_2 s^2\right)\right]\left\{\begin{array}{l} -F_2(s) + \left(1/\chi_{ij}^{\Psi}\right)\times \\ \times \left[d_{mi}\Psi_m(s) - \left[\gamma/\text{sh}(l\gamma)\right]\left[\text{ch}(l\gamma)\Xi_2(s) - \Xi_1(s)\right]\right] \end{array}\right\},$$

Copyright © Society for Science and Education United Kingdom

where $\chi_{ij}^{\Psi}=s_{ij}^{\Psi}/S_0$, $v_{mi}=\begin{Bmatrix} d_{33},d_{31},d_{15} \\ d_{33},d_{31},d_{15} \end{Bmatrix}$, $\Psi_m=\begin{Bmatrix} E_3,E_1 \\ H_3,H_1 \end{Bmatrix}$, $s_{ij}^{\Psi}=\begin{Bmatrix} s_{33}^{E},s_{11}^{E},s_{55}^{E} \\ s_{33}^{H},s_{11}^{H},s_{55}^{H} \end{Bmatrix}$, $\gamma=\begin{Bmatrix} \gamma^{E} \\ \gamma^{H} \end{Bmatrix}$.

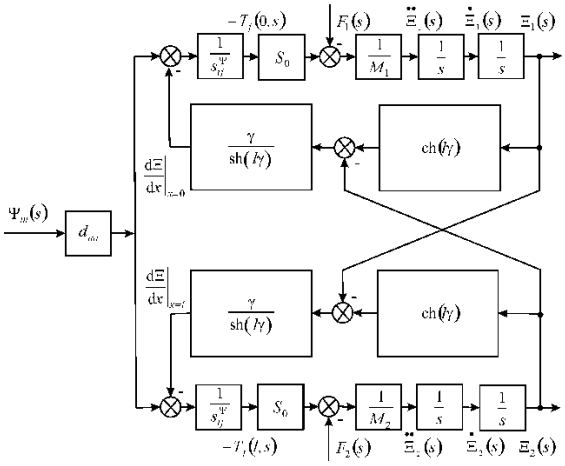


Figure 1. Block diagram of electromagnetoelastic actuator for nanoscience and nanotechnology

The system of the equations for the Laplace transform of the displacements of two faces of the electromagnetoelastic actuator is received after the transformation (11) in the form

$$\Xi_1(s)=W_{11}(s)\Psi_m(s)+W_{12}(s)F_1(s)+W_{13}(s)F_2(s);$$

$$\Xi_2(s)=W_{21}(s)\Psi_m(s)+W_{22}(s)F_1(s)+W_{23}(s)F_2(s). \quad (12)$$

Therefore, the matrix equation with the matrix transfer function has the form

$$(\Xi(s))=(W(s))(P(s));. \quad (13)$$

$$(\Xi(s))=\begin{pmatrix}\Xi_1(s)\\ \Xi_2(s)\end{pmatrix},\ (W(s))=\begin{pmatrix}W_{11}(s) & W_{12}(s) & W_{13}(s)\\ W_{21}(s) & W_{22}(s) & W_{23}(s)\end{pmatrix},\ (P(s))=\begin{pmatrix}\Psi_m(s)\\ F_1(s)\\ F_2(s)\end{pmatrix},$$

where $(\Xi(s))$ is the column-matrix of the Laplace transforms of the displacements, $(W(s))$ is the matrix transfer function, $(P(s))$ is the column-matrix of the Laplace transforms of the control parameter and the forces.

Therefore, the matrix equation for the displacements is received from (13) in the form

$$\begin{pmatrix}\Xi_1(s)\\ \Xi_2(s)\end{pmatrix}=\begin{pmatrix}W_{11}(s) & W_{12}(s) & W_{13}(s)\\ W_{21}(s) & W_{22}(s) & W_{23}(p)\end{pmatrix}\begin{pmatrix}\Psi_m(s)\\ F_1(s)\\ F_2(s)\end{pmatrix}, \quad (14)$$

where $W_{11}(s)$, $W_{12}(s)$, $W_{13}(s)$, $W_{21}(s)$, $W_{22}(s)$, $W_{23}(s)$ are the transfer functions of the elements in the matrix transfer function in the following form

$$W_{11}(s)=\Xi_1(s)/\Psi_m(s)=d_{mi}\left[M_2\chi_{ij}^{\Psi}s^2+\gamma\mathrm{th}(l\gamma/2)\right]/A_{ij}; \quad (15)$$

$$W_{21}(s)=\Xi_2(s)/\Psi_m(s)=d_{mi}\left[M_1\chi_{ij}^{\Psi}s^2+\gamma\mathrm{th}(l\gamma/2)\right]/A_{ij};$$

$$W_{12}(s)=\Xi_1(s)/F_1(s)=-\chi_{ij}^{\Psi}\left[M_2\chi_{ij}^{\Psi}s^2+\gamma/\mathrm{th}(l\gamma)\right]/A_{ij};$$

$$\begin{aligned}&W_{13}(s)=\Xi_1(s)/F_2(s)\\&=W_{22}(s)=\Xi_2(s)/F_1(s)=\left[\chi_{ij}^{\Psi}\gamma/\mathrm{sh}(l\gamma)\right]/A_{ij};\end{aligned}$$

$$W_{23}(s)=\Xi_2(s)/F_2(s)=-\chi_{ij}^{\Psi}\left[M_1\chi_{ij}^{\Psi}s^2+\gamma/\mathrm{th}(l\gamma)\right]/A_{ij};$$

$$\chi_{ij}^{\Psi}=s_{ij}^{\Psi}/S_0;$$

$$\begin{aligned}&A_{ij}=M_1M_2\left(\chi_{ij}^{\Psi}\right)^2s^4+\left\{(M_1+M_2)\chi_{ij}^{\Psi}/\left[c^{\Psi}\mathrm{th}(l\gamma)\right]\right\}s^3\\&+\left[(M_1+M_2)\chi_{ij}^{\Psi}\alpha/\mathrm{th}(l\gamma)+1/\left(c^{\Psi}\right)^2\right]s^2+2\alpha s/c^{\Psi}+\alpha^2.\end{aligned}$$

The block diagram of the piezoactuator is obtained for the reverse and direct piezoelectric effects. The equation of the direct piezoeffect [7 – 9, 13, 14] for the piezoactuator has the form

$$D_m=d_{mi}T_i+\varepsilon_{mk}^{E}E_k, \quad (16)$$

where D_m is the electric induction; ε_{mk}^{E} is the dielectric permittivity at $E=\mathrm{const}$; $k=1,2,3$ is the index. The block diagram of the piezoactuator on Figure 2 is obtained with account the counter electromotive force from the direct piezoeffect.

From the equation of direct piezoeffect (15) at $E=\mathrm{const}$ the equation for the coefficient k_d of the direct piezoeffect has the form

$$k_d=\frac{I_{\dot{\Xi}_n}(s)}{\dot{\Xi}_n(s)}=\frac{d_{mi}S_0}{\delta s_{ij}^{E}}, \quad n=1,2, \quad (17)$$

where $I_{\dot{\Xi}_n}(s)$, $\dot{\Xi}_n(s)$ are the Laplace transform of the current, the velocity of the face 1 or 2 for the piezoactuator; n is number of the face piezoactuator. From (16) the equation for the Laplace transform of the voltage for the negative feedback of the piezoactuator has the form

$$U_{\dot{\Xi}_n}(s)=\frac{d_{mi}S_0R}{\delta s_{ij}^{E}}\dot{\Xi}_n(s), \quad n=1,2. \quad (18)$$

The block diagram of the piezoactuator is received with using the inverse and direct piezoelectric effects on Figure 2 from (11) after transformations the block diagram of the actuator on Figure 1 with adding the equation (18).

Copyright © Society for Science and Education United Kingdom

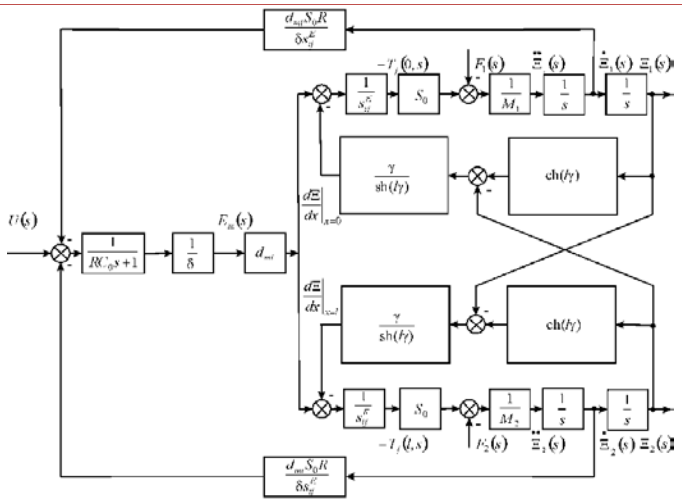


Figure 2. Block diagram of piezoactuator for nanoscience and nanotechnology

The coefficient k_d of the direct piezoeffect and the coefficient k_r of the reverse piezoeffect of the piezoactuator are obtained in the following form

$$k_d = k_r = \frac{d_{mi} S_0}{\delta s_{ij}^E}. \tag{19}$$

The structural diagram of the piezoactuator on Figure 3 with the lumped parameters for one rigidly fixed face at $n = 1$ under the elastic-inertial load are received after replacing the hyperbolic cotangent on two members of the power series.

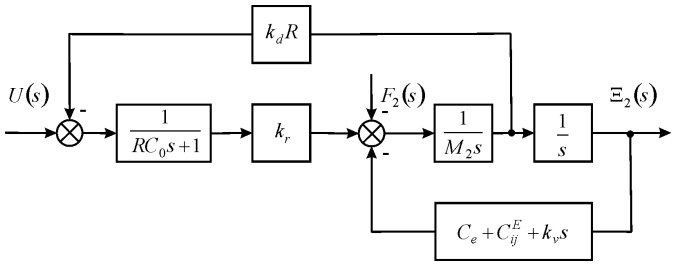


Figure 3. Block diagram of piezoactuator at elastic-inertial load for nanoscience and nanotechnology

The transfer function for the structural diagram of the piezoactuator is obtained for the lumped parameters at $R = 0$ on Figure 3 in the form

$$W(s) = \frac{\Xi_2(s)}{U(s)} = \frac{k_r}{M_2 s^2 + k_v s + C_{ij}^E + C_e}, \tag{20}$$

where $\Xi_2(s)$, $U(s)$ are Laplace transformations of the displacement of the face and the voltage of the piezoactuator.

Then the transfer function for the piezoactuator at $R = 0$ has the form

$$W(s) = \frac{\Xi_2(s)}{U(s)} = \frac{d_{mi}(l/\delta)}{\left(1 + C_e / C_{ij}^E\right)\left(T_t^2 s^2 + 2T_t \xi_t s + 1\right)}; \tag{21}$$

$$T_t = \sqrt{M_2 / \left(C_{ij}^E + C_e\right)},\ \xi_t = k_v \Big/ \left(2\left(C_{ij}^E + C_e\right)\sqrt{M_2\left(C_{ij}^E + C_e\right)}\right),\ C_{ij}^E = S_0 / \left(s_{ij}^E l\right) = 1/\left(\chi_{ij}^E l\right).$$

The transfer function of the transverse piezoactuator at $R = 0$ has the form

$$W(s) = \frac{\Xi_2(s)}{U(s)} = \frac{d_{31}\, h/\delta}{\left(1 + C_e / C_{11}^E\right)\left(T_t^2 s^2 + 2T_t \xi_t s + 1\right)}; \tag{22}$$

$$T_t = \sqrt{M_2 / \left(C_e + C_{11}^E\right)},\ \xi_t = \alpha h^2 C_{11}^E \Big/ \left(3c^E \sqrt{M\left(C_e + C_{11}^E\right)}\right);\ C_{11}^E = S_0 / \left(s_{11}^E h\right) = 1/\left(\chi_{11}^E h\right),$$

where h, δ, T_t, ξ_t are the height, the thickness, the time constant and the attenuation coefficient of the piezoactuator. At d_{31} = 2.5·10^{-10} m/V, h/δ =20, M_2 = 1 kg, C_{11}^E = 2·10^7 N/m, C_e = 0.2·10^7 N/m, U = 110 V for the transverse piezoactuator from ceramic PZT with one rigidly fixed face are obtained the time constant T_t = 0.21·10^{-3} s and for time $t \to \infty$ the displacement ξ_2 = 500 nm.

3 Characteristics of Electromagnetoelastic actuator

The static characteristics of the electromagnetoelastic actuator with fixe one face are received in the form the mechanical and control characteristics for control systems in nanoscience and nanotechnology. From (1) the mechanical characteristic of the electromagnetoelastic actuator has form the characteristic $S_i\left(T_j\right)$ the relative displacement from the mechanical stress or $\Delta l(F)$ the displacement from the force at $\Psi = \text{const}$. The mechanical characteristic has the following form

$$S_i\big|_{\Psi=\text{const}} = d_{mi}\Psi_m\big|_{\Psi=\text{const}} + s_{ij}^{\Psi} T_j\,. \tag{23}$$

From (1) the control characteristic of the electromagnetoelastic actuator has the form the characteristic $S_i(\Psi_m)$ the relative displacement from the control parameter in the form electric E_m or magnetic H_m field strength or $\Delta l(U)$ the displacement from the voltage at $T = \text{const}$. The control characteristic has the form

$$S_i\big|_{T=\text{const}} = d_{mi}\Psi_m + s_{ij}^{\Psi} T_j\big|_{T=\text{const}}\,. \tag{24}$$

The mechanical characteristic of the electromagnetoelastic actuator is received in the following equation

$$\Delta l = \Delta l_{\max}\left(1 - F/F_{\max}\right), \tag{25}$$

where $\Delta l_{\max}$ is the maximum displacement for $F = 0$ and $F_{\max}$ is the maximum force for $\Delta l = 0$.

The maximum displacement of the electro magneto elastic actuator has the form

$$\Delta l_{\max} = d_{mi}\Psi_m l\,, \tag{26}$$

where l is the length of the electromagnetoelastic actuator. We have the length of the piezoactuator in the form the thickness at the longitudinal piezoeffect, the height at the transverse piezoeffect and the width at the shear piezoeffect.

Copyright © Society for Science and Education United Kingdom

The maximum mechanical stress of the electromagnetoelastic actuator has the form

$$T_{j\max} = d_{mi}\Psi_m / s_{ij}^{\Psi} . \quad (27)$$

Then the maximum force of the electromagnetoelastic actuator for control systems is determined in the following form

$$F_{\max} = T_{j\max} S_0 = d_{mi}\Psi_m S_0 / s_{ij}^{\Psi} . \quad (28)$$

For the transverse piezoactuator the maximum displacement and the maximum force are obtained in the form

$$\Delta l_{\max} = d_{31} E_3 l , \quad F_{\max} = d_{31} E_3 S_0 / s_{11}^{E} \quad (29)$$

At d_{31} = 2.5·10^{-10} m/V, E_3 = 3·10^5 V/m, l = 2·10^{-2} m, S_0 = 1·10^{-5} m^2, s_{11}^{E} = 15·10^{-12} m^2/N for the transverse piezoactuator from ceramic PZT the maximum displacement $\Delta l_{\max}$ = 1.5 μm and the maximum force $F_{\max}$ = 50 N are received on Figure 4.

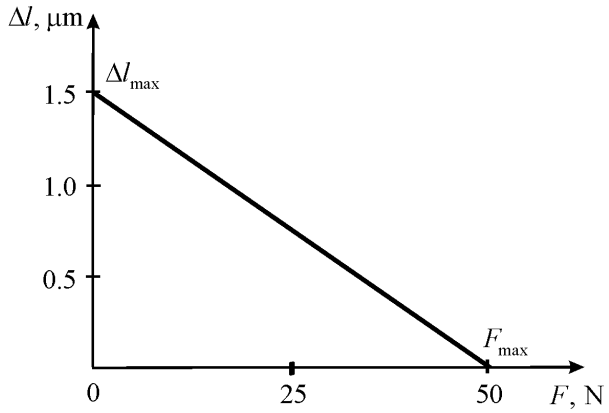


Figure 4. Mechanical characteristic of transverse piezoactuator for nanoscience and nanotechnology

The regulation characteristic of the electromagnetoelastic actuator at elastic force has the form

$$\frac{\Delta l}{l} = d_{mi}\Psi_m - \frac{s_{ij}^{\Psi} C_e}{S_0}\Delta l , \quad (30)$$

$$F = C_e \Delta l .$$

From (30) the displacement of the electromagnetoelastic actuator for elastic load has the form

$$\Delta l = \frac{d_{mi} l \Psi_m}{1 + C_e / C_{ij}^{\Psi}} , \quad (31)$$

$$C_{ij}^{\Psi} = S_0 / \left(s_{ij}^{\Psi} l\right).$$

From (31) the regulation characteristic of the transverse piezoactuator has the following form

$$\Delta l = \frac{(d_{31}\, h/\delta)U}{1 + C_e / C_{11}^E} = k_{31}^U U ,$$

$$k_{31}^U = (d_{31}\, h/\delta) / (1 + C_e / C_{11}^E),$$

where k_{33}^U is the transfer coefficient. At d_{31} = 2.5·10^{-10} m/V, h/δ =10, C_{11}^E = 4·10^7 N/m, C_e = 1·10^7 N/m, U = 100 V for the transverse piezoactuator from ceramic PZT the transfer coefficient k_{33}^U = 2 nm/V and the displacement Δl = 200 nm are obtained. The experimental and calculated values for the piezoactuator are in agreement up to an accuracy of 10%.

4 Conclusion

The block diagram of the electromagnetoelastic actuator is received with the mechanical parameters the displacement and the force the for control systems in nanoscience and nanotechnology. The mechanical and the control characteristics of the electromagnetoelastic actuator are obtained. The block diagram of the electromagnetoelastic actuator is used for the reflection the transformation of electrical energy into mechanical energy of the actuator, in contrast to Cady's and Mason's electrical equivalent circuits of piezotransducer.

The block diagram of the electromagnetoelastic actuator is determined by solved the electromagnetoelasticity equation and the second order linear ordinary differential equation with boundary conditions. The matrix transfer function of the electromagnetoelastic actuator and the transfer functions of the piezoactuators are obtained for nanomechatronics systems in nanoscience and nanotechnology.

The block diagram of the piezoactuator is received with using the reverse and direct piezoelectric effects. The mechanical characteristic and the regulation characteristic of the piezoactuator are obtained for control systems. The maximum displacement and the maximum force of the piezoactuator are determined for the mechanical characteristic.

REFERENCES

[1]. Schultz, J., Ueda, J., Asada, H., *Cellular actuators*. Oxford: Butterworth-Heinemann Publisher, 2017. 382 p.

[2]. Afonin, S.M., *Absolute stability conditions for a system controlling the deformation of an elecromagnetoelastic transduser*. Doklady mathematics, 2006. 74(3): p. 943-948, doi:10.1134/S1064562406060391.

[3]. Zhou, S., Yao, Z., *Design and optimization of a modal-independent linear ultrasonic motor.* IEEE transaction on ultrasonics, ferroelectrics, and frequency control, 2014. 61(3): p. 535-546, doi:10.1109/TUFFC.2014.2937.

[4]. Przybylski, J., *Static and dynamic analysis of a flextensional transducer with an axial piezoelectric actuation*. Engineering structures, 2015. 84: p. 140-151, doi:10.1016/j.engstruct.2014.11.025.

Copyright © Society for Science and Education United Kingdom

[5]. Ueda, J., Secord, T., Asada, H.H., *Large effective-strain piezoelectric actuators using nested cellular architecture with exponential strain amplification mechanisms*. IEEE/ASME transactions on mechatronics, 2010. 15(5): p. 770-782, doi:10.1109/TMECH.2009.2034973.

[6]. Karpelson, M., Wei, G.-Y., Wood, R.J., *Driving high voltage piezoelectric actuators in microrobotic applications. Sensors and actuators* A: Physical, 2012. 176: p. 78-89, doi:10.1016/j.sna.2011.11.035.

[7]. Afonin, S.M., *Block diagrams of a multilayer piezoelectric motor for nano- and microdisplacements based on the transverse piezoeffect*. Journal of computer and systems sciences international, 2015. 54(3): p. 424-439, doi:10.1134/S1064230715020021.

[8]. Afonin, S.M., *Structural parametric model of a piezoelectric nanodisplacement transduse*r. Doklady physics, 2008. 53(3) p. 137-143, doi:10.1134/S1028335808030063.

[9]. Afonin, S.M., *Solution of the wave equation for the control of an elecromagnetoelastic transduser*. Doklady mathematics, 2006. 73(2), p. 307-313, doi:10.1134/S1064562406020402.

[10]. Cady W.G., *Piezoelectricity: An introduction to the theory and applications of electromechancial phenomena in crystals*. New York, London: McGraw-Hill Book Company, 1946. 806 p.

[11]. *Physical acoustics*: *Principles and methods. Vol.1. Part A. Methods and devices*. Mason, W., Editor, New York: Academic Press, 1964. 515 p.

[12]. Zwillinger, D., *Handbook of differential equations*. Boston: Academic Press, 1989. 673 p.

[13]. Afonin, S.M., *Structural-parametric model and transfer functions of electroelastic actuator for nano- and microdisplacement*. Chapter 9 in *Piezoelectrics and nanomaterials: Fundamentals, developments and applications*. Parinov, I.A., Editor, New York: Nova Science, 2015. p. 225-242.

[14]. Afonin, S.M., *A structural-parametric model of electroelastic actuator for nano- and microdisplacement of mechatronic system*. Chapter 8 in *Advances in nanotechnology. Volume 19*. Bartul, Z., Trenor, J., Editors, New York: Nova Science, 2017. p. 259-284.

[15]. Afonin, S.M., Nano- and micro-scale piezomotors. Russian engineering research, 2012. 32(7-8): p. 519-522, doi:10.3103/S1068798X12060032.

[16]. Afonin, S.M., *Elastic compliances and mechanical and adjusting characteristics of composite piezoelectric transducers*. Mechanics of solids, 2007. 42(1): p. 43-49, doi:10.3103/S0025654407010062.

[17]. Afonin, S.M., *Static and dynamic characteristics of a multi-layer electroelastic solid*. Mechanics of solids, 2009. 44(6): p. 935-950, doi:10.3103/S002565440.

[18]. Afonin, S.M., *Static and dynamic characteristics of multilayered electromagnetoelastic transducer of nano- and micrometric movements*. Journal of computer and systems sciences international, 2010. 49(1): p. 73-85, doi:10.1134/S106423071.

[19]. Afonin, S.M., *Structural-parametric model electromagnetoelastic actuator nanodisplacement for mechatronics*. International journal of physics, 2017. 5(1): p. 9-15, doi: 10.12691/ijp-5-1-27.

[20]. Afonin, S.M., *Structural-parametric model multilayer electromagnetoelastic actuator for nanomechatronics*. International journal of physics, 2019. 7(2): p. 50-57, doi:10.12691/ijp-7-2-3.

[21]. Afonin SM (2018) *Structural-parametric model of electromagnetoelastic actuator for nanomechanics*. Actuators, 2018. 7(1): 1-9, doi: 10.3390/act7010006.

[22]. Afonin, S.M., *Structural-parametric model and diagram of a multilayer electromagnetoelastic actuator for nanomechanics*. Actuators, 2019. 8(3): 1-14, doi: 10.3390/act8030052.

[23]. Afonin, S.M., *A block diagram of electromagnetoelastic actuator nanodisplacement for communications systems*. Transactions on networks and communications, 2018. 6(3): p. 1-9, doi:10.14738/tnc.63.4641.

[24]. Afonin, S.M., *Decision matrix equation and block diagram of multilayer electromagnetoelastic actuator micro and nanodisplacement for communications systems*, Transactions on networks and communications, 2019. 7(3): p. 11-21, doi:10.14738/tnc.73.6564.

[25]. Afonin, S.M., *Condition absolute stability control system of electromagnetoelastic actuator for communication equipment*. Transactions on networks and communications, 2020. 8(1): p. 8-15, doi:10.14738/tnc.81.7775.

[26]. Afonin, S.M., *Structural scheme actuator for nano research*. COJ Reviews and Research, 2020. 2(5): p. 1-3, doiI:10.31031/COJRR.2020.02.000548.

[27]. Afonin, S.M., *Structural–parametric model electroelastic actuator nano- and microdisplacement of mechatronics systems for nanotechnology and ecology research*. MOJ ecology and environmental sciences, 2018. 3(5): p. 306–309. doi:10.15406/mojes.2018.03.00104.

[28]. Afonin, S.M., *Structural-parametric model of electro elastic actuator for nanotechnology and biotechnology.* Journal of pharmacy and pharmaceutics, 2018. 5(1): p. 8-12, doi:10.15436/2377-131.

[29]. Afonin, S.M., *Condition absolute stability of control system with electro elastic actuator for nano bioengineering and microsurgery*. Surgery and case studies open access journal, 2019. 3(3): p. 307–309, doi:10.32474/SCSOAJ.2019.03.000165.

[30]. *Springer Handbook of Nanotechnology*. Bhushan, B., Editor, Springer, Berlin, New York, 2004. 1222 p.

Copyright © Society for Science and Education United Kingdom